

Hyperfine-assisted fast electric control of dopant nuclear spins in semiconductors

Péter Boross,¹ Gábor Széchenyi,¹ and András Pályi^{2,3,*}

¹*Institute of Physics, Eötvös University, 1518 Budapest, Hungary*

²*Department of Physics, Budapest University of Technology and Economics, 1111 Budapest, Hungary*

³*MTA-BME Condensed Matter Research Group, Budapest University of Technology and Economics, 1111 Budapest, Hungary*

Nuclear spins of dopant atoms in semiconductors are promising candidates as quantum bits, due to the long lifetime of their quantum states. Conventionally, coherent control of nuclear spins is done using ac magnetic fields. Using the example of a phosphorus atom in silicon, we theoretically demonstrate that hyperfine interaction can enhance the speed of magnetic control: the electron on the donor amplifies the ac magnetic field felt by the nuclear spin. Based on that result, we show that hyperfine interaction also provides a means to control the nuclear spin efficiently using an ac electric field, in the presence of intrinsic or artificial spin-orbit interaction. This electric control scheme is especially efficient and noise-resilient in a hybrid dot-donor system holding two electrons in the presence of an inhomogeneous magnetic field. The mechanisms proposed here could be used as building blocks in nuclear-spin-based electronic quantum information architectures.

Introduction. The nuclear spin of a phosphorus (P) atom in silicon (Si) is a highly coherent two-level system[1, 2], and hence is a competitive candidate for representing a qubit in quantum information processing[3, 4]. Resonant control of a single nuclear-spin qubit have been demonstrated using ac magnetic fields in the spirit of nuclear magnetic resonance[5]; initialization and read-out can be performed using the donor electron spin[6, 7].

Similarly to the case of electron spin qubits, for nuclear spins it would also be beneficial to substitute the ac magnetic control with ac electric control: this could lead to simplified sample design, spatially confined control fields, lower power requirements, higher qubit densities, shorter gate times, and an opportunity to couple nuclear spins electrically to each other or to electromagnetic resonators[8, 9]. One challenge to achieve these for the P:Si system is that P has a spin-1/2 nuclear spin, which does not couple directly to the electric field[10]. Nevertheless, recent activities advance toward this goal by proposing a combined electric-magnetic control scheme in a dot-donor system[8], by demonstrating electric control of the hyperfine interaction[11] and nuclear spin states in an ensemble of nuclear spins in Si[9] and in a single-molecule magnet[12, 13].

In this work, we propose and analyze a mechanism to control the P nuclear spin efficiently using ac electric fields. The mechanism relies on hyperfine interaction: we utilize the donor-bound electron as a quantum transducer between the electric field and the nuclear spin. Actually, this transducer effect can be exploited to speed up qubit control already in the case of magnetic drive, which is a conceptually simpler scenario; therefore, first we discuss how it works in the case of magnetic drive.

Hyperfine-assisted magnetic control of the P:Si nuclear spin. First, consider a single ionized P atom in Si, in a homogeneous static magnetic field B_0 along the z axis, driven resonantly by an ac magnetic field along the x axis, with amplitude B_{ac} and frequency f . Dynamics is described by the Hamiltonian $H_{B,n} + H_{d,n}(t)$, where

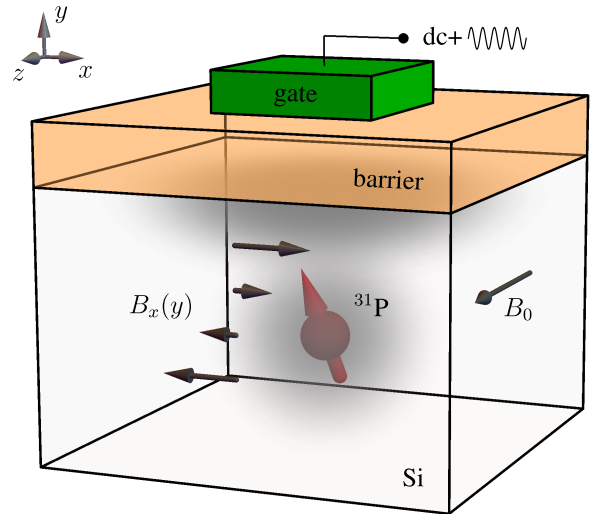


FIG. 1. **Electrically driven nuclear spin resonance of a phosphorus atom in a silicon dot-donor system.** The dc gate voltage is used to balance the donor's electron on a bonding orbital (gray cloud) of the artificial molecule formed by the dot-donor system. The ac gate-voltage component oscillates the electron vertically. Due to these charge oscillations and the presence of the inhomogeneous magnetic field $B_x(y)$, the electron spin on the donor acquires an oscillating x component, which drives the nuclear spin (red arrow) via the hyperfine interaction.

$H_{B,n} = -h\gamma_n B_0 I_z$ and $H_{d,n}(t) = -h\gamma_n B_{ac} \sin(2\pi ft) I_x$, $\gamma_n = 17.23 \text{ MHz/T}$ is the nuclear gyromagnetic ratio, and $\mathbf{I} = (I_x, I_y, I_z)$ is the spin-1/2 nuclear spin operator. When driven resonantly ($f = f_L^{(i)} \equiv \gamma_n B_0$), the nuclear spin performs complete Rabi oscillations with Rabi frequency $f_R^{(i)} = \frac{1}{2} \gamma_n B_{ac}$.

Consider how this result changes when the donor is not ionized, but neutral, i.e., it has a single electron (1e) occupying the ground-state donor orbital. The Hamilto-

nian is

$$H(t) = H_{B,e} + H_{B,n} + H_{\text{hf}} + H_{\text{d,e}}(t) + H_{\text{d,n}}(t). \quad (1)$$

Here, $H_{B,e} = h\gamma_e B_0 S_z$, $H_{\text{hf}} = \mathbf{AS} \cdot \mathbf{I}$, and $H_{\text{d,e}} = h\gamma_e B_{\text{ac}} \sin(2\pi ft) S_x$, whereas $\gamma_e = 27.97 \text{ GHz/T}$ is the electron gyromagnetic ratio, $A/h = 117 \text{ MHz}$ is the hyperfine coupling strength, and $\mathbf{S} = (S_x, S_y, S_z)$ is the electron spin operator. Consider the experimentally relevant case[5] when the electronic Zeeman splitting dominates the hyperfine strength, $h\gamma_e B_0 \gg A$. Assume that the system is in its ground state, well approximated by the state $|\downarrow\uparrow\rangle$ with the electron spin pointing down and the nuclear spin pointing up, before the driving starts. Then, the nuclear Larmor frequency is $f_L^{(\downarrow)} \approx \frac{A}{2\hbar} + \gamma_n B_0 \ll \gamma_e B_0$. Upon driving at the nuclear Larmor frequency, due to $f = f_L^{(\downarrow)} \ll \gamma_e B_0$, the electron spin will adiabatically follow the direction of the instantaneous magnetic field: $\langle \mathbf{S} \rangle_t \approx -\frac{1}{2} \left(\frac{B_{\text{ac}}}{B_0} \sin(2\pi ft), 0, 1 \right)$. This electron spin dynamics will in turn create an additional transverse driving field (Knight field) on the nuclear spin via the hyperfine interaction: $H'_{\text{d,n}}(t) = A \langle S_x \rangle_t I_x = -\frac{AB_{\text{ac}}}{2B_0} \sin(2\pi ft) I_x$. As a consequence of this extra driving term, the Rabi frequency is increased with respect to the ionized case: $f_R^{(\downarrow)} = \frac{1}{2} \left(\gamma_n + \frac{A}{2\hbar B_0} \right) B_{\text{ac}}$. A similar consideration shows that for an up-spin electron, the Rabi frequency is $f_R^{(\uparrow)} = \frac{1}{2} \left(\gamma_n - \frac{A}{2\hbar B_0} \right) B_{\text{ac}}$.

An analogous effect in nitrogen-vacancy defects in diamond was termed ‘hyperfine-enhanced nuclear gyromagnetic ratio’, and was characterized theoretically and experimentally[14–18]. For the P:Si system, a straightforward experimental proof of this hyperfine-assisted nuclear spin control could be obtained by extending the analysis presented in Fig. 3 of [5]. E.g., using the nuclear-spin Rabi oscillations of the ionized P, the ac magnetic field amplitude at the donor position can be determined, which can be used to predict the nuclear-spin Rabi frequency for the neutral P with an up-spin electron.

Hyperfine-assisted electric control of the P:Si nuclear spin. The previous mechanism suggests the possibility of ac electric control, in the case when the ac electric field can modulate the local instantaneous Knight field at the position of the P nucleus. We demonstrate that this modulation can be achieved in a two-site system controlled by gate electrodes, e.g., in a dot-donor system[19–25], in the presence of an inhomogeneous magnetic field[26].

First, we consider the case when a single electron is confined in the dot-donor system (Fig. 1). The orbital degree of freedom is described in the two-dimensional Hilbert space spanned by the ground-state orbital localized in the dot ($|i\rangle$) and that localized on the donor ($|d\rangle$). The distance between the centers of these orbitals is d . The magnetic-field inhomogeneity is characterized by the field gradient β , and the magnetic field takes the values $(\pm \frac{\beta d}{2}, 0, B_0)$ on the dot and the donor, respectively.

Then, the minimal model of this setup[8, 20, 23] can be written as

$$H = H_o + H_{B,e} + H_{B,n} + H_{\text{hf}} + H_{\mu,e} + H_{\mu,n} + H_d(t), \quad (2)$$

with the orbital Hamiltonian $H_o = \frac{U}{2} \sigma_z + \frac{V_t}{2} \sigma_x$, the hyperfine interaction $H_{\text{hf}} = An_d \mathbf{S} \cdot \mathbf{I}$, the inhomogeneous magnetic field

$$H_{\mu,e} = h\gamma_e \frac{\beta d}{2} \sigma_z S_x \quad (3a)$$

$$H_{\mu,n} = h\gamma_n \frac{\beta d}{2} I_x, \quad (3b)$$

and the electric drive $H_d(t) = \frac{U_{\text{ac}}}{2} \sigma_z \sin(2\pi ft)$. Here, U is the gate-tunable on-site energy difference between $|i\rangle$ and $|d\rangle$, V_t is the tunnel coupling between them, $\sigma_{x,y,z}$ are the Pauli matrices acting on the orbital degree of freedom (e.g., $\sigma_z = |i\rangle\langle i| - |d\rangle\langle d|$), $n_d \equiv (1 - \sigma_z)/2$ is the electron number on the donor, and $U_{\text{ac}} = eE_{\text{ac}}d$ is the on-site energy difference induced by an ac electric field E_{ac} along the dot-donor axis, created via an ac voltage excitation of the gate electrode. The 8 energy eigenvalues of this Hamiltonian are shown in Fig. 2a as a function of the on-site energy difference U (see caption for parameters); the lowest two branches labelled $|\downarrow\rangle$ and $|\uparrow\rangle$ correspond to the basis states of the nuclear-spin qubit.

To illustrate that electric driving $H_d(t)$ results in a time-dependent Knight field for the donor nuclear spin, and thereby induces nuclear-spin Rabi oscillations, we consider a simple case: when the electron is balanced at the tipping point between the $|i\rangle$ and $|d\rangle$ orbitals ($U = 0$, gray vertical line in Fig. 2a)[20], the electronic Zeeman splitting equals the tunnel coupling ($h\gamma_e B_0 = V_t$), and these energy scales well exceed all other energy scales, including the drive frequency. Then, similarly to the case of magnetic driving discussed above, the electron dynamics is adiabatic. Assuming that the electron is in its ground state when the driving starts, the time dependence of the electron wave function $\psi(t)$ can be described by the instantaneous ground state of $H_o + H_{B,e} + H_{\mu,e} + H_d(t)$. We obtain an explicit expression for $\psi(t)$ using second-order perturbation theory in $H_{\mu,e} + H_d(t)$, and use that to express the time-dependent Knight field $\mathbf{b}(t)$ acting on the nuclear spin via the hyperfine Hamiltonian:

$$\bar{H}_{\text{hf}}(t) = A \langle \psi(t) | n_d \mathbf{S} | \psi(t) \rangle \cdot \mathbf{I} \equiv \mathbf{b}(t) \cdot \mathbf{I}. \quad (4)$$

After dropping high-harmonic terms with frequencies above f , we find $\mathbf{b}(t) = \mathbf{b}_0 + \mathbf{b}_{\text{ac}} \sin(2\pi ft)$. Keeping only the terms up to second (third) order in the small energy scales A , $h\gamma_e \beta d$, U_{ac} for \mathbf{b}_0 (\mathbf{b}_{ac}), we obtain

$$\mathbf{b}_0 = \begin{pmatrix} \frac{A(h\gamma_e \beta d)}{16V_t} \\ 0 \\ -\frac{A}{4} \end{pmatrix}, \quad \mathbf{b}_{\text{ac}} = \begin{pmatrix} \frac{A(h\gamma_e \beta d)U_{\text{ac}}}{8V_t^2} \\ 0 \\ -\frac{AU_{\text{ac}}}{4V_t} \end{pmatrix}, \quad (5)$$

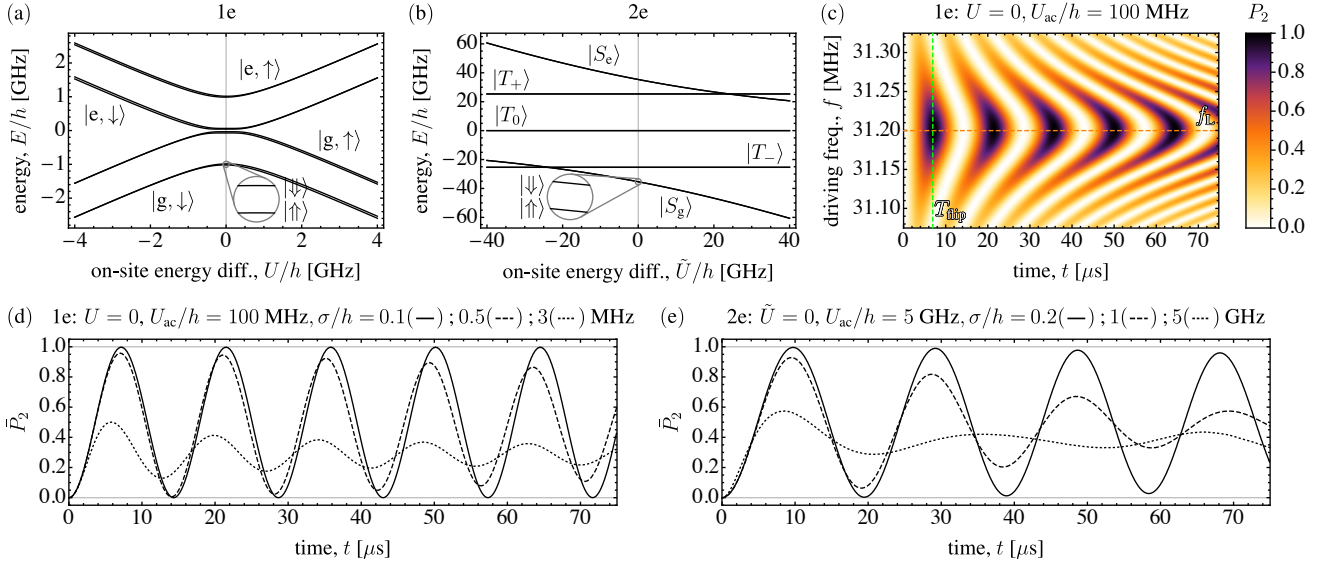


FIG. 2. **Electrically driven nuclear-spin Rabi oscillations and their damping due to charge noise.** (a,b) shows the energy level structure of the single-electron (1e) and two-electron (2e) setups, as functions of energy detuning from the (1,0)-(0,1) and (1,1)-(0,2) tipping points, respectively. (c) Nuclear-spin Rabi oscillations induced by electrically driving a single electron at the tipping point $U = 0$. Time-dependent occupation probability $P_2(t, f)$ of the excited state of the nuclear-spin qubit shows the standard Chevron pattern of magnetic resonance, in the absence of noise. Green dashed line shows the spin-flip time $T_{\text{flip}} = 1/(2f_R)$ predicted by Eq. (6). Orange dashed line shows the numerically calculated nuclear-spin Larmor frequency f_L , i.e., the separation between the two lowest eigenvalues of the static Hamiltonian. (d,e) Damping of the nuclear-spin Rabi oscillations due to different strengths of charge noise (σ), in the 1e and 2e setups, for resonant drive. $\bar{P}_2(t)$ is the noise-averaged occupation probability of the excited state of the nuclear-spin qubit, see Eq. (7). The 2e setup is three orders of magnitude more resilient to charge noise than the 1e setup. Parameters: $\beta = 0.47$ mT/nm, $d = 15$ nm. (a,c,d) $V_t/h = 1$ GHz, $B_0 = 35.7$ mT (b,e) $V_t/h = 50$ GHz, $B_0 = 906.5$ mT.

from which we express the third-order result for the Rabi frequency on resonance as

$$hf_R = \frac{1}{2} \left| \frac{\mathbf{b}_0}{b_0} \times \mathbf{b}_{\text{ac}} \right| = \frac{A(h\gamma_e\beta d)U_{\text{ac}}}{32V_t^2}. \quad (6)$$

This is the central result of this work, demonstrating that electric driving (U_{ac}) can indeed induce nuclear-spin Rabi oscillations when assisted by hyperfine interaction (A) and the inhomogeneous magnetic field (β).

The nuclear-spin Larmor frequency at the tipping point is $f_L \approx A/(4h) \approx 30$ MHz, and from experimentally feasible parameters ($d = 15$ nm, $U_{\text{ac}}/h = 100$ MHz corresponding to $E_{\text{ac}} = 27.6$ V/m), we estimate a nuclear-spin Rabi frequency $f_R \approx 72$ kHz upon resonant driving. This Rabi frequency corresponds to an effective coupling constant $f_R/E_{\text{ac}} \approx 3 \times 10^6$ kHz $\mu\text{m}/\text{V}$, which is more than 4 orders of magnitude larger than the electric coupling determined experimentally for the P ensemble in bulk Si, attributed to electronic g-tensor modulation[9][27]. Key ingredients in this giant enhancement are: (i) the energy denominator which has to be bridged by the perturbation mechanisms is much lower in the dot-donor hybrid (it is $hV_t \approx 4.1$ μeV in our example) than for a P donor in bulk (~ 10 meV), (ii) the spatial extension of the electronic orbitals is much larger in the dot-donor system ($d = 15$ nm) than in an isolated donor (~ 1 nm).

To demonstrate the reliability of the above quantitative considerations, we numerically solved the 8×8 time-dependent Schrödinger equation for the model defined in Eq. (2). The initial state was the ground state of the nuclear-spin qubit, i.e., the ground state of the static Hamiltonian $H - H_d(t)$. In Fig. 2c, we show a ‘Chevron’ plot, i.e., the time-dependent occupation probability P_2 of the first excited state of the static Hamiltonian (the excited qubit basis state). The plot reveals regular Rabi oscillations of the nuclear spin. The horizontal line shows the numerically obtained nuclear Larmor frequency, i.e., the difference between the second and first eigenvalues of the static Hamiltonian. The vertical line shows the spin-flip time $1/(2f_R)$, evaluated from Eq. (6), matching well with the probability peak of the numerical data.

Electrical potential fluctuations are expected to affect these Rabi oscillations, and thereby hinder their experimental observability, and their application as single-qubit gates. The effect of noise is illustrated in Fig. 2d, where damped Rabi oscillations are shown for different strengths of the noise. Noise is modelled as a random static on-site energy difference between the interface and the donor sites[20], $H_n = \frac{U_n}{2}\sigma_z$, with a Gaussian probability distribution $\rho_\sigma(U_n)$ characterized by its standard deviation σ . Each curve $\bar{P}_2(t)$ in Fig. 2d is derived by

computing the coherent time evolution of the excited-state occupation probability $P_2(t, U_n)$, and averaging via

$$\bar{P}_2(t) = \int_{-\infty}^{\infty} dU_n P_2(t, U_n) \rho_{\sigma}(U_n). \quad (7)$$

We evaluated this integral numerically, using an equidistant grid with 101 points in the $[-2.5, 2.5]\sigma$ interval.

The key observation in Fig. 2d is that already the first Rabi-oscillation peak is strongly damped at a noise level $\sigma/h = 3$ MHz (dotted). Based on recent experiments, we expect that the noise level in Si devices[20, 28] is of the order of $\sigma_{\text{exp}}/h = 0.2$ GHz, which suggests that the observation of these Rabi oscillations requires a significant reduction of charge noise.

This strong noise susceptibility has a simple interpretation, offering a vastly improved alternative setup. At the tipping point, charge noise is effective in displacing the electron, therefore (i) changes the electron's overlap with the P nucleus, hence (ii) changes the effective strength of the hyperfine interaction, and therefore (iii) changes the z-directional Knight field, leading to (iv) a change in the nuclear-spin Larmor frequency [29]. This is apparent in Eq. (5): the detuning-induced shift of the Larmor frequency is $\delta f_L = -AU_n/(4V_t)$. Since noise shifts the Larmor frequency, the electric drive becomes off-resonant for many of the noise realizations, hence the noise-averaged Rabi oscillations become incomplete. A solution to this problem, leading to orders of magnitude improvement of the quality of Rabi oscillations, is based on using two electrons in the dot-donor system instead of one. We show here that in such a two-electron (2e) setup, the modulation of the transverse Knight field via electric driving remains significant, whereas the modulation of the longitudinal Knight field can be suppressed compared to the 1e case, providing efficient control of the nuclear-spin qubit together with resilience to charge noise.

For the demonstration, we assume that (see, e.g., [21]), two electrons occupy the dot-donor system, and the on-site energy difference is tuned to the tipping point between the (1,1) and (0,2) configurations, where (N_i, N_d) denotes when N_i (N_d) electrons reside at the interface (donor). The Hamiltonian is a natural 2e generalization of the 1e Hamiltonian given above[30], and is represented by a 10×10 matrix due to the 5 (2) different electron (nuclear) spin states $|S\rangle, |T_+\rangle, |T_0\rangle, |T_-\rangle, |S_{02}\rangle$ ($|\uparrow\rangle, |\downarrow\rangle$). Fig. 2b shows the dependence of the energy spectrum on the parameter \tilde{U} representing the on-site energy detuning from the (1,1)-(0,2) tipping point, using values $V_t/h = 50$ GHz and $B = 906.5$ mT. We choose the nuclear-spin qubit as the two energy eigenstates associated to the lowest-energy line labelled $|S_g\rangle$. Figure 2e shows that the 2e setup is more than three orders of magnitude more resilient to charge noise than the 1e setup. Our data (solid) predicts that multiple high-quality Rabi oscillations can be observed for the estimated experimen-

tal noise level $\sigma_{\text{exp}}/h = 0.2$ GHz. (See [30] for further details.)

Generalizations. In an actual experiment, the inhomogeneous magnetic field can be provided by a micromagnet[31]. However, incorporating the magnet in the setup complicates fabrication. We argue that, similarly to the case of electrically driven electron spin resonance[32, 33] it is possible to avoid that complication if spin-orbit interaction is significant in the sample, as highlighted for the Si conduction band in recent experiments[34–36]. In a simple two-site model[23, 37] of the dot-donor setup, spin-orbit interaction enters the electronic Hamiltonian as a spin-dependent tunnel coupling, e.g., $H_{\text{so}} = V_s \sigma_y S_y$. Note that it is important that the spin projection appearing here is not parallel to the external magnetic field. It is straightforward to see that H_{so} plays a role analogous to the inhomogeneous magnetic field, and hence able to mediate interaction between the driving electric field and the nuclear spin. We demonstrate this for the tipping point $U = 0$ in the 1e setup, and weak spin-orbit interaction $V_s \ll V_t$. Using the unitary transformation $W = e^{i\phi\sigma_z S_y}$ on the electronic degrees of freedom with $\phi = \arctan(V_s/V_t)$, the spin-dependent tunneling term can be eliminated, and the same transformation renders the magnetic field inhomogeneous. The leading-order terms in the transformed Hamiltonian read $W(H_o + H_{\text{so}})W^\dagger \approx V_t \sigma_x/2$, and $WH_{B,e}W^\dagger \approx h\gamma_e B_0(S_z - \frac{V_s}{V_t}\sigma_z S_x)$. Comparing this result with Eq. (3a) reveals that the spin-orbit interaction is equivalent to a magnetic field gradient $2\frac{B_0}{d}\frac{V_s}{V_t}$. This implies a spin-orbit-mediated nuclear Rabi frequency of $f_R = \frac{AV_s U_{\text{acc}}}{16hV_t^2} \approx 72$ kHz for the parameters listed above, using a spin-orbit interaction strength $V_s = 0.1V_t$. Another mechanism via which spin-orbit interaction influences electron dynamics is g-factor anisotropy[20, 23, 38], which could also facilitate nuclear spin dynamics.

The interaction mechanisms we propose here between the nuclear-spin qubit and electric fields offers potential pathways toward scalable quantum information processing: it allows dispersive qubit readout using electromagnetic resonators, and two-qubit logical operations[20] either via dipole-dipole interaction of the donor-bound electrons, or via photon-mediated interaction through an electromagnetic resonator. Note that the latter, photon-mediated interaction usually requires that the Larmor frequency f_L of the qubit and the mode frequency f_{res} of the resonator are close to each other, whereas the nuclear Larmor frequency in our setup (few tens of MHz) is way below the typical mode frequency of high-quality superconducting resonators (few GHz). This difficulty could be resolved using two-photon Raman processes, where an auxiliary classical driving field with frequency $\approx f_{\text{res}} - f_L$ compensates the mismatch between the qubit and resonator energy quanta. Such an arrangement has been analyzed in [8], where the classical driving field was magnetic; that could be substituted by all-electric driv-

ing in the presence of an inhomogeneous magnetic field or spin-orbit interaction.

Conclusions. In conclusion, we propose an efficient scheme to control dopant nuclear spins in engineered semiconductor nanostructures with ac electric fields. The scheme relies on an interplay of (intrinsic or artificial) spin-orbit coupling, hyperfine interaction, and the molecular states in a dot-donor system, and provides orders of magnitude enhancement of the coupling strength between the nuclear spin and the electric field, as compared to the measured value in bulk. We predict that even in the presence of realistic charge noise, high-quality nuclear-spin Rabi oscillations can be detected in an electrically driven two-electron dot-donor system. The mechanism we propose could serve as an important building block in scalable nuclear-spin-based quantum information processing architectures.

Acknowledgments. We thank W. A. Coish, T. Fehér, A. Morello, A. Sigillito, G. Tosi and L. Vandersypen for useful discussions. This research was supported by the National Research Development and Innovation Office of Hungary within the Quantum Technology National Excellence Program (Project No. 2017-1.2.1-NKP-2017-00001), and Grants 105149, 124723, and 108676. B. P. and A. P. were supported by the New National Excellence Program of the Ministry of Human Capacities.

* Corresponding author: palyi@mail.bme.hu

- [1] J. T. Muhonen, J. P. Dehollain, A. Laucht, F. E. Hudson, R. Kalra, T. Sekiguchi, K. M. Itoh, D. N. Jamieson, J. C. McCallum, A. S. Dzurak, and A. Morello, *Nat Nano* **9**, 986 (2014).
- [2] K. Saeedi, S. Simmons, J. Z. Salvail, P. Dluhy, H. Riemann, N. V. Abrosimov, P. Becker, H.-J. Pohl, J. J. L. Morton, and M. L. W. Thewalt, *Science* **342**, 830 (2013).
- [3] B. E. Kane, *Nature* **393**, 133 (1998).
- [4] F. A. Zwanenbourg, A. S. Dzurak, A. Morello, M. Simmons, L. Hollenberg, G. Klimeck, S. Rogge, S. Copper-smith, and M. Eriksson, *Rev. Mod. Phys.* **85**, 961 (2013).
- [5] J. J. Pla, K. Y. Tan, J. P. Dehollain, W. H. Lim, J. J. L. Morton, F. A. Zwanenbourg, D. N. Jamieson, A. S. Dzurak, and A. Morello, *Nature* **496**, 334 (2013).
- [6] A. Morello, J. J. Pla, F. A. Zwanenbourg, K. W. Chan, K. Y. Tan, H. Huebl, M. Mottonen, C. D. Nugroho, C. Yang, J. A. van Donkelaar, A. D. C. Alves, D. N. Jamieson, C. C. Escott, L. C. L. Hollenberg, R. G. Clark, and A. S. Dzurak, *Nature* **467**, 687 (2010).
- [7] J. J. Pla, K. Y. Tan, J. P. Dehollain, W. H. Lim, J. J. L. Morton, D. N. Jamieson, A. S. Dzurak, and A. Morello, *Nature* **489**, 541 (2012).
- [8] G. Tosi, F. A. Mohiyaddin, S. Tenberg, A. Laucht, and A. Morello, “Robust electric dipole transition at microwave frequencies for nuclear spin qubits in silicon,” ArXiv:1706.08095 (unpublished).
- [9] A. J. S. an A. M. Tyryshkin, T. Schenkel, A. A. Houck, and S. A. Lyon, “Electrically driving nuclear spin qubits with microwave photonic bandgap resonators,” ArXiv:1701.06650 (unpublished).
- [10] C. P. Slichter, *Principles of Magnetic Resonance* (Harper & Row, New York, 1963).
- [11] A. Laucht, J. T. Muhonen, F. A. Mohiyaddin, R. Kalra, J. P. Dehollain, S. Freer, F. E. Hudson, M. Veldhorst, R. Rahman, G. Klimeck, K. M. Itoh, D. N. Jamieson, J. C. McCallum, A. S. Dzurak, and A. Morello, *Science Advances* **1** (2015), 10.1126/sciadv.1500022.
- [12] S. Thiele, F. Balestro, R. Ballou, S. Klyatskaya, M. Ruben, and W. Wernsdorfer, *Science* **344**, 1135 (2014).
- [13] C. Godfrin, A. Ferhat, R. Ballou, S. Klyatskaya, M. Ruben, W. Wernsdorfer, and F. Balestro, *Phys. Rev. Lett.* **119**, 187702 (2017).
- [14] L. Childress, M. V. Gurudev Dutt, J. M. Taylor, A. S. Zibrov, F. Jelezko, J. Wrachtrup, P. R. Hemmer, and M. D. Lukin, *Science* **314**, 281 (2006).
- [15] B. Smeltzer, J. McIntyre, and L. Childress, *Phys. Rev. A* **80**, 050302 (2009).
- [16] S. Sangtawesin, T. O. Brundage, and J. R. Petta, *Phys. Rev. Lett.* **113**, 020506 (2014).
- [17] M. Chen, M. Hirose, and P. Cappellaro, *Phys. Rev. B* **92**, 020101 (2015).
- [18] S. Sangtawesin, C. A. McLellan, B. A. Myers, A. C. B. Jayich, D. D. Awschalom, and J. R. Petta, *New Journal of Physics* **18**, 083016 (2016).
- [19] G. P. Lansbergen, R. Rahman, C. J. Wellard, I. Woo, J. Caro, N. Collaert, S. Biesemans, G. Klimeck, L. C. L. Hollenberg, and S. Rogge, *Nat. Phys.* **4**, 656 (2008).
- [20] G. Tosi, F. A. Mohiyaddin, V. Schmitt, S. Tenberg, R. Rahman, G. Klimeck, and A. Morello, *Nature Communications* **8**, 450 (2017).
- [21] M. Urdampilleta, A. Chatterjee, C. C. Lo, T. Kobayashi, J. Mansir, S. Barraud, A. C. Betz, S. Rogge, M. F. Gonzalez-Zalba, and J. J. L. Morton, *Phys. Rev. X* **5**, 031024 (2015).
- [22] P. Harvey-Collard, N. T. Jacobson, M. Rudolph, J. Dominguez, G. A. Ten Eyck, J. R. Wendt, T. Pluym, J. K. Gamble, M. P. Lilly, M. Pioro-Ladrière, and M. S. Carroll, *Nature Communications* **8**, 1029 (2017).
- [23] P. Boross, G. Széchenyi, and A. Pályi, *Nanotechnology* **27**, 314002 (2016).
- [24] P. Harvey-Collard, B. DAnjou, M. Rudolph, N. T. Jacobson, J. Dominguez, G. A. T. Eyck, J. R. Wendt, T. Pluym, M. P. Lilly, W. A. Coish, M. Pioro-Ladrière, and M. S. Carroll, “High-fidelity single-shot readout for a spin qubit via an enhanced latching mechanism,” ArXiv:1703.02651 (unpublished).
- [25] M. Rudolph, P. Harvey-Collard, R. Jock, N. Jacobson, J. Wendt, T. Pluym, J. Dominguez, G. Ten-Eyck, R. Manginell, M. Lilly, and M. Carroll, “Coupling MOS Quantum Dot and Phosphorus Donor Qubit Systems,” ArXiv:1705.05887 (unpublished).
- [26] Similar setups have been studied for the purpose of electric control of electron spins[31, 39].
- [27] Further comparisons: our coupling strength estimate is approximately 3 orders of magnitude larger than that determined experimentally for the single-molecule magnet in Ref. [12], and a factor of 50 smaller than that theoretically estimated for the combined magnetic-electric two-photon Raman scheme in Ref. [8].
- [28] B. M. Freeman, J. S. Schoenfeld, and H. W. Jiang, *Appl. Phys. Lett.* **108**, 253108 (2016).

- [29] The electrically induced change in the nuclear-spin Larmor frequency is responsible for a further effect: an anomalous Bloch-Siegert shift[30, 40–42].
- [30] Supplementary Material.
- [31] M. Pioro-Ladriere, T. Obata, Y. Tokura, Y. S. Shin, T. Kubo, K. Yoshida, T. Taniyama, and S. Tarucha, *Nat Phys* **4**, 776 (2008).
- [32] K. C. Nowack, F. H. L. Koppens, Y. V. Nazarov, and L. M. K. Vandersypen, *Science* **318**, 1430 (2007).
- [33] V. N. Golovach, M. Borhani, and D. Loss, *Phys. Rev. B* **74**, 165319 (2006).
- [34] M. Veldhorst, R. Ruskov, C. H. Yang, J. C. C. Hwang, F. E. Hudson, M. E. Flatté, C. Tahan, K. M. Itoh, A. Morello, and A. S. Dzurak, *Phys. Rev. B* **92**, 201401 (2015).
- [35] A. Corna, L. Bourdet, R. Maurand, A. Crippa, D. Kotekar-Patil, H. Bohuslavskyi, R. Laviéville, L. Hutin, S. Barraud, X. Jehl, M. Vinet, S. De Franceschi, Y.-M. Niquet, and M. Sanquer, *npj Quantum Information* **4**, 6 (2018).
- [36] R. M. Jock *et al.*, “Probing low noise at the MOS interface with a spin-orbit qubit,” ArXiv:1707.04357 (unpublished).
- [37] J. Danon and Y. V. Nazarov, *Phys. Rev. B* **80**, 041301 (2009).
- [38] R. Rahman, S. H. Park, T. B. Boykin, G. Klimeck, S. Rogge, and L. C. L. Hollenberg, *Phys. Rev. B* **80**, 155301 (2009).
- [39] Y. Tokura, W. G. van der Wiel, T. Obata, and S. Tarucha, *Phys. Rev. Lett.* **96**, 047202 (2006).
- [40] F. Bloch and A. Siegert, *Phys. Rev.* **57**, 522 (1940).
- [41] J. H. Shirley, *Phys. Rev.* **138**, B979 (1965).
- [42] J. Romhányi, G. Burkard, and A. Pályi, *Phys. Rev. B* **92**, 054422 (2015).

Supplementary material for

“Hyperfine-assisted fast electric control of dopant nuclear spins in semiconductors”

Péter Boross¹, Gábor Széchenyi¹, and András Pályi^{2,3}

¹ *Institute of Physics, Eötvös University, 1518 Budapest, Hungary*

² *Department of Physics, Budapest University of Technology and Economics, 1111 Budapest, Hungary*

³ *MTA-BME Condensed Matter Research Group, Budapest University of Technology and Economics, 1111 Budapest, Hungary*

SUPPLEMENTARY NOTE 1: MODEL AND RESULTS FOR THE TWO-ELECTRON SETUP

Here, we provide further details of the two-electron (2e) setup discussed in the main text. Our goal is to express the Knight field that acts on the nuclear spin due to the presence of the two electrons, and from that to deduce the parameter dependence of the nuclear-spin Rabi frequency upon resonant electric driving, in a similar fashion as done in the main text for the single-electron (1e) setup, see Eqs. (4), (5), (6).

The 2e Hamiltonian is a straightforward generalization of the 1e Hamiltonian introduced in Eq. (2) of the main text. Due to Coulomb repulsion between the electrons, we introduce an extra 2e on-site Coulomb term:

$$H_C = \frac{U_C}{2} [n_i(n_i - 1) + n_d(n_d - 1)], \quad (\text{S1})$$

where U_C is its the Coulomb energy, and we choose to have the same Coulomb energy on both the $|i\rangle$ and $|d\rangle$ orbitals for simplicity. We keep a single orbital per site, resulting in a 6-dimensional Hilbert space. We use the standard singlet-triplet basis, with states denoted as $|S(1,1)\rangle \equiv |S\rangle$, $|T_+(1,1)\rangle \equiv |T_+\rangle$, $|T_0(1,1)\rangle \equiv |T_0\rangle$, $|T_-(1,1)\rangle \equiv |T_-\rangle$, $|S(0,2)\rangle \equiv |S_{02}\rangle$, $|S(2,0)\rangle \equiv |S_{20}\rangle$. Here, (N_i, N_d) denotes the charge configuration where N_i (N_d) electrons reside at the interface (donor).

We focus on the case where the electrons are tuned by the dc gate voltage to the vicinity of the (1,1)-(0,2) tipping point. There, the state $|S_{20}\rangle$ can be neglected due to the large Coulomb energy U_C . Then, the terms of the complete (electronic+nuclear) Hamiltonian of the 1e setup in Eq. (2) of the main text are expressed for the 2e setup in the product basis $\{|S\rangle, |T_+\rangle, |T_0\rangle, |T_-\rangle, |S_{20}\rangle\} \otimes$

$\{|\downarrow\rangle, |\uparrow\rangle\}$ as

$$H_o = -\tilde{U} |S_{02}\rangle \langle S_{02}| + \frac{V_t}{\sqrt{2}} (|S\rangle \langle S_{02}| + \text{h.c.}), \quad (\text{S2a})$$

$$H_{B,e} = h\gamma_e B_0 (|T_+\rangle \langle T_+| - |T_-\rangle \langle T_-|), \quad (\text{S2b})$$

$$H_{\mu,e} = \frac{1}{\sqrt{2}} h\gamma_e \frac{\beta d}{2} (|T_-\rangle \langle S| - |T_+\rangle \langle S| + \text{h.c.}), \quad (\text{S2c})$$

$$H_{\text{hf}} = \frac{A}{2} (-|T_0\rangle \langle S| - |S\rangle \langle T_0| - |T_-\rangle \langle T_-| + |T_+\rangle \langle T_+|) I_z + \frac{A}{\sqrt{2}} [(|T_+\rangle \langle S| + |T_+\rangle \langle T_0| + |T_0\rangle \langle T_-| - |S\rangle \langle T_-|) I_+ + \text{h.c.}], \quad (\text{S2d})$$

$$H_d(t) = -U_{ac} |S_{02}\rangle \langle S_{02}| \sin(2\pi f t), \quad (\text{S2e})$$

Note that here H_o incorporates the Coulomb repulsion H_C as well, and we have defined the detuning parameter $\tilde{U} = U - U_C$, which characterizes the on-site energy difference measured from the (1,1)-(0,2) tipping point.

To obtain the time-dependent Knight field $\mathbf{b}(t)$ felt by the donor nuclear spin in the 2e setup, we use the same adiabatic approximation that lead us to Eqs. (4) and (5) of the main text in the 1e setup. For the 2e setup, we find

$$\mathbf{b}_0 = \begin{pmatrix} \frac{A(h\gamma_e\beta d)}{8\delta} \\ 0 \\ h\gamma_n B_0 + \frac{A^2}{4\delta} \end{pmatrix}, \quad \mathbf{b}_{ac} = \begin{pmatrix} -\frac{A(h\gamma_e\beta d)U_{ac}}{16\delta^2} \\ 0 \\ -\frac{A^2 U_{ac}}{32\delta^2} \end{pmatrix} \quad (\text{S3})$$

where $\delta = \frac{V_t}{\sqrt{2}} - h\gamma_e B_0$ is the detuning of $|S_g\rangle$ and $|T_-\rangle$ and we assume that $\delta \ll V_t$. Here, $|S_g\rangle$ ($|S_e\rangle$) is the ground (excited) state of the two-electron orbital Hamiltonian (S2a), see the energy spectrum in Fig. 2b in the main text. The Rabi frequency can be written as

$$hf_R = \frac{A(h\gamma_e\beta d)U_{ac}}{32\delta^2} \quad (\text{S4})$$

in the $\delta \ll V_t$ limit. This result is almost identical to the Rabi frequency in the 1e case, Eq. (6) of the main text, with the only difference that here δ plays the role of V_t . The highly improved noise resilience of the 2e setup demonstrated by Fig. 2e is due to the fact that longitudinal component of the ac Knight field [that is, the third component of \mathbf{b}_{ac} in Eq. (S3)], is of third order

in the small energy scales, in contrast to the 1e setup, where the longitudinal ac Knight field is of second order.

The dc and ac Knight fields in (S3) are derived using perturbation theory for a 10-level system. The key point in the result is the existence of a transverse Knight field (the first component of \mathbf{b}_0), which gains time dependence due to the ac electric excitation, resulting in a finite first component of \mathbf{b}_{ac} , and thereby allows for nuclear-spin control via electrical driving. Here we show a minimal model which contains these essential features. The key observation, which is somewhat counterintuitive, is the following: a 2e singlet state $|S\rangle$, weakly mixed with a longitudinally polarized triplet $|T_-\rangle$, produces a dominantly transverse Knight field. To see this, consider $|\psi\rangle = \sqrt{1-\varepsilon}|S\rangle + \sqrt{\varepsilon}|T_-\rangle$, where $\varepsilon \ll 1$. The Knight field on the donor, felt by the donor nuclear spin, is

$$\langle\psi|n_d\mathbf{S}|\psi\rangle = -(\sqrt{\varepsilon/2}, 0, \varepsilon/2). \quad (\text{S5})$$

In other words, even though we mix a state producing no Knight field ($|S\rangle$) and a state producing purely longitudinal Knight field ($|T_-\rangle$), the mixture produces a dominantly transversal Knight field. Importantly, this observation is harnessed in the 2e setup discussed in the main text. The reason for choosing the particular parameter set of Fig. 2b and e is to create a situation where the $|S_g\rangle$ and $|T_-\rangle$ are close to each other in energy but far from the other electronic states, and thereby allowing $|S_g\rangle$ to perturbatively hybridize with $|T_-\rangle$ due to the mixing effect of the inhomogeneous magnetic field. This perturbative hybridization then leads to the transverse Knight-field components proportional to the magnetic-field gradient β in Eq. (S3).

SUPPLEMENTARY NOTE 2: BLOCH-SIEGERT SHIFT OF THE RESONANCE FREQUENCY

A key difference between the 1e and 2e setups is the strength of the longitudinal ac Knight field: in the 1e setup, it arises as a strong, second-order term, see Eq. (5), whereas in the 2e setup, it is a weaker, third-order term, see Eq. (S3). One dramatic consequence of this difference is that the nuclear-spin Rabi oscillations of the 1e setup are much less resilient to charge noise, as shown in Fig. 2d,e, and discussed in the main text. Another observable consequence of this difference is the appearance of an unexpectedly large drive-strength-dependent shift of the resonance frequency in the 1e case, which we refer to as an *anomalous Bloch-Siegert shift*. As we show below, this Bloch-Siegert shift of the resonance frequency becomes pronounced as the working point is detuned from the tipping point between the interface and the donor.

Figure S1b,d,f show the qubit-flip probability (color coded) in the 1e setup, for three different dc gate volt-

ages, whose equilibrium charge distributions are depicted in Fig. S1a,c,e, respectively. The black horizontal lines in Fig. S1b,d,f indicate the Larmor frequency of the nuclear-spin qubit, corresponding to the energy splitting of the undriven qubit. Fig. S1b and f reveal that the apparent resonance frequency does not match the Larmor frequency when the electron is detuned from the ionization point. The deviation increases with increasing drive strength (not shown). This effect is known as the Bloch-Siegert shift (BSS) in magnetic resonance [41,42], and was also analyzed in electrically driven spin resonance [43]. In magnetic resonance, as long as the driving field is weaker than the static field, and as long as the fundamental resonance ($f \approx f_L$) is considered, the BSS is always positive and much smaller than the power broadening of the resonance [41,42] (i.e., the broadening of the resonance along the driving-frequency direction), and therefore hardly resolvable. In our case, however, the BSS is positive in Fig. S1b but negative in Fig. S1f, moreover, the BSS is comparable to the power broadening. Because of these unconventional features, we refer to this as an anomalous BSS.

This anomalous BSS can be explained as a dynamical consequence of the electric modulation of the hyperfine strength. The simple argument is that the electric drive modulates the electron weight $n_d(U + U_{ac} \sin(2\pi ft))$ on the donor, which in turn modulates the nuclear Larmor frequency via the hyperfine interaction $H_{hf} = An_d\mathbf{S} \cdot \mathbf{I}$, as the nuclear Larmor frequency has a Knight-field contribution of $An_d/2$. Taking the time average of this contribution after second-order expansion in U_{ac}/U , we obtain $hf_{\text{BSS}} = AU_{ac}^2 n_d''(U)/8$. Noting that in the ground state, the electron weight on the donor is $n_d(U) \approx \frac{1}{2} \left(1 + U/\sqrt{U^2 + V_t^2}\right)$, we conclude that

$$hf_{\text{BSS}} \approx -\frac{3}{16} \frac{AU_{ac}^2 UV_t^2}{(U^2 + V_t^2)^{5/2}}. \quad (\text{S6})$$

This result is third order in the perturbative parameters (A, U_{ac}), just like the Rabi frequency in Eq. (6), which explains why the BSS is comparable to the power broadening in this setup. A good agreement is shown between this analytical result, represented as the horizontal green dashed lines in Fig. S1, and the numerical data. Note that this anomalously strong BSS is absent in the 2e case (not shown) discussed in Fig. 2, even when a finite detuning \tilde{U} is applied.

As a final remark, we note that it is possible to generalize our analytical Rabi frequency result Eq. (6) of the main text. That result was obtained for the 1e setup, for the special case when the working point is the tipping point between the interface and donor (denoted by the vertical gray line at $U = 0$ in Fig. 2a of the main text). Allowing for a finite on-site energy detuning $U \neq 0$ from the tipping point, and following the same method as described in the main text, we obtain the generalization of

1e: $V_t = 1$ GHz, $B_0 = 35.8$ mT, $U_{ac} = 100$ MHz

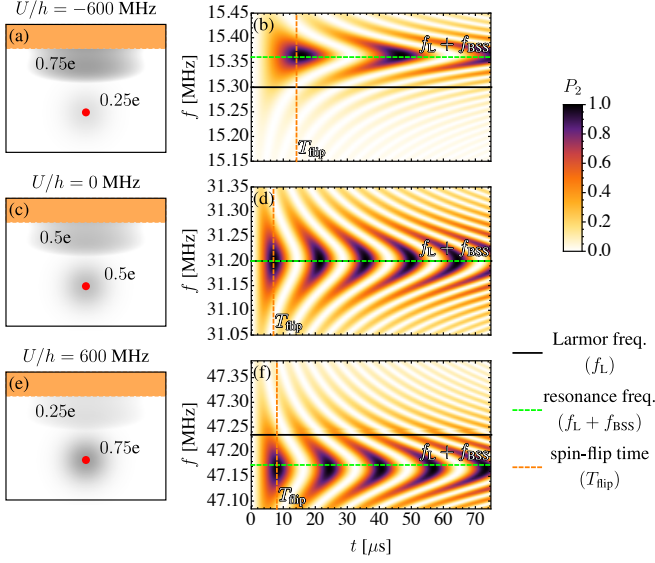


FIG. S1. Anomalous Bloch-Siegert shift in electrically driven nuclear spin resonance with a single electron. (a,c,e) Charge distribution of the electron in the dot-donor system, for a single electron, for three different values of the gate-induced dc electric field $U/(ed)$. (b,d,f) Nuclear-spin Rabi oscillations: occupation probability $P_2(t, f)$ of the excited basis state of the nuclear-spin qubit as a function of time t and drive frequency f , for the charge distribution shown in a/c/e, respectively. Solid black lines show the numerically calculated nuclear-spin Larmor frequency f_L , corresponding to the separation between the two lowest-energy eigenvalues of the static Hamiltonian. Green dashed lines show the resonance frequency obtained as the sum of f_L and the Bloch-Siegert shift f_{BSS} given by Eq. (S6). Orange vertical lines show the spin-flip time $1/(2f_R)$ predicted by Eq. (S7).

Eq. (6) as

$$hf_R = \frac{A(h\gamma_e\beta d)U_{ac}V_t \left(U + V_t + \sqrt{U^2 + V_t^2} \right)}{16(U^2 + V_t^2) \left(V_t + \sqrt{U^2 + V_t^2} \right)^2}. \quad (\text{S7})$$

In Fig. S1b,d,f, the vertical dashed orange lines indicate the spin-flip time $T_{\text{flip}} = 1/(2f_R)$ based on Eq. (S7), showing a satisfactory agreement with the peak positions of numerically obtained excited-state occupation probabilities.

In conclusion, here we have demonstrated that the apparent resonance frequency in the single-electron setup depends strongly on the drive strength when ac electrical driving is used. This effect is interpreted as an anomalous Bloch-Siegert shift: in contrast to the Bloch-Siegert shift in conventional paramagnetic resonance, here the apparent detuning of the resonance frequency can be comparable to the power broadening of the resonance, and can have an unconventional, negative sign.